HHS Public Access

Author manuscript

Contrast Media Mol Imaging. Author manuscript; available in PMC 2016 March 01.

Published in final edited form as:

Contrast Media Mol Imaging. 2015 March ; 10(2): 135–143. doi:10.1002/cmmi.1609.

Specificity of lectin-immobilized fluorescent nanospheres for colorectal tumors in a mouse model which more resembles the clinical disease

Tokio Kitamura[a], **Shinji Sakuma**[a,*], **Moe Shimosato**[a], **Haruki Higashino**[a], **Yoshie Masaoka**[a], **Makoto Kataoka**[a], **Shinji Yamashita**[a], **Ken-ichiro Hiwatari**[b], **Hironori Kumagai**[b], **Naoki Morimoto**[a,b], **Seiji Koike**[b], **Etsuo Tobita**[b], **Robert M. Hoffman**[c,d], **John C. Gore**[e], and **Wellington Pham**[e,*]

[a]Faculty of Pharmaceutical Sciences, Setsunan University, 45-1 Nagaotoge-cho, Hirakata, Osaka 573-0101, Japan

[b]Life Science Materials Laboratory, ADEKA Co., 7-2-34 Higashiogu, Arakawa-ku, Tokyo 116-8553, Japan

[c]AntiCancer, Inc., 7917 Ostrow Street, San Diego, CA 92111, USA

[d]Department of Surgery, University of California at San Diego, La Jolla, CA 92103-8220, USA

[e]Institute of Imaging Science, Medical Center, Vanderbilt University, 1161 21st Ave. S. Nashville, TN 37232-2310, USA

Abstract

We are investigating an imaging agent that enables real-time and accurate diagnosis of early colorectal cancer at the intestinal mucosa by colonoscopy. The imaging agent is peanut agglutinin-immobilized polystyrene nanospheres with surface poly(N-vinylacetamide) chains encapsulating coumarin 6. Intracolonically-administered lectin-immobilized fluorescent nanospheres detect tumor-derived changes through molecular recognition of lectin for the terminal sugar of cancer-specific antigens on the mucosal surface. The focus of this study was to evaluate imaging abilities of the nanospheres in animal models that reflect clinical environments. We previously developed an orthotopic mouse model with human colorectal tumors growing on the mucosa of the descending colon to more resemble the clinical disease. The entire colon of the mice in the exposed abdomen was monitored in real-time with an *in vivo* imaging apparatus. Fluorescence from the nanospheres was observed along the entire descending colon after intracolonical administration of them from the anus. When the luminal side of the colon was washed with PBS, most of the nanospheres drained away. However, fluorescence persisted in areas where the cancer cells were implanted. Histological evaluation demonstrated that tumors were present in the mucosal epithelia where the nanospheres fluoresced. In contrast, no fluorescence was observed when control mice without tumors were tested. The lectin-immobilized fluorescent nanospheres were tumor specific and bound to tumors even after vigorously washing. The nanospheres non-specifically bound to normal mucosa were easily removed through mild washing. Results indicate

[*]Corresponding author 1 (Shinji Sakuma). Tel.: +81-72-866-3124; Fax: +81-72-866-3126; sakuma@pharm.setsunan.ac.jp. Corresponding author 2 (Wellington Pham). Tel.: +1-615-936-7621; Fax: +1-615-322-0734; wellington.pham@Vanderbilt.Edu.

that the nanospheres accompanied by colonoscopy will be a clinically-valuable diagnostic tool for the early stage primary colon carcinoma.

Keywords

imaging; optical imaging; contrast agent; fluorescent probes; fluorescent nanospheres; colonoscopy; colorectal cancer; biorecognition; molecular recognition

1. Introduction

Colonoscopy has been effectively used for screening colorectal cancer due to its ability to provide a definitive diagnosis [1–3]. Just like any other cancers, the early detection of colorectal cancer is critical for successful treatment. Colorectal cancer initially develops in the mucous membrane of the large intestine. The cancer, which remains in the mucous membrane or only minimally invades the submucosal tissues without vessel invasion, is often removed through the colonoscopy procedure. Alternatively, when the cancer is detected in the early stage, it can be treated by minimally invasive operation, known as endoscopic mucosal resection (EMR) [4].

Magnifying endoscopy and novel imaging strategies for endoscopy such as narrow band imaging enabled physicians to detect small changes on the mucosal surface of the large intestine [5]. Most colorectal cancer can be prevented through the detection and removal of premalignant polypoid lesions [6]. However, the efficacy of current endoscopic screening, which is based on morphological changes through a macroscopic view of the mucosal surface, is limited due to lack of diagnosis at the molecular level. Conventional endoscopy is not generally suitable for flat and depressed neoplasms [7]. Patients with chronic inflammatory bowel disease face with increased risk of developing malignancy due to undetected dysplastic lesions [8]. There is an unmet need for improved methods for detecting early changes in high-risk individuals. Hsiung et al. who identified heptapeptide sequence with high affinity for fresh human colonic adenomas have been investigating the heptapeptide sequence-conjugated fluorescent probes accompanied by colonoscopy for the above-mentioned purpose [9]. Furthermore, accurate differentiation of neoplastic mucosal changes in real-time still remains a significant challenge. Tissues that look like abnormal are sampled under endoscopic observation. Successive histological evaluation of the samples is prerequisite for the definitive diagnosis of the cancer. There is also a need for developing a colonoscopic imaging agent that enables physicians to diagnose early stage primary colon carcinoma on the mucosal surface in real-time and enforce EMR simultaneously. The imaging agent definitely becomes a useful diagnostic tool for tiny tumors that are currently undetectable or difficult to detect under endoscopic observation.

We previously designed a non-absorbable imaging agent capable of being administered intracolonically for the purpose of colonoscopy [10–16]. The imaging agent consists of peanut (*Arachis hypogaea*) agglutinin (PNA)-immobilized polystyrene nanospheres with surface poly(N-vinylacetamide) (PNVA) chains encapsulating coumarin 6 (Fig. 1). The Thomsen-Friedenreich (TF) antigen is specifically expressed on the mucosal side of colorectal cancer cells [17–21]. The antigen is also a malignancy index of colorectal cancer

[22]. PNA is immobilized on the nanosphere surface as a targeting moiety that binds to the TF antigen through molecular recognition of its terminal sugar: β-D-galactosyl-(1-3)-N-acetyl-D-galactosamine (Gal-β(1-3)GalNAc) [23], which is masked by oligosaccharide side chain extension or by sialylation in normal cells. We previously observed that PNVA rarely adhered to the intestinal mucosa due to its strong hydrophilicity [24–25]. This polymer chain is localized on the nanosphere surface to enhance the specificity of PNA by reducing nonspecific interactions between the nanospheres and normal tissues. Coumarin 6 is encapsulated into the nanosphere core as the fluorescent dye that produces an endoscopically-detectable fluorescence intensity.

We have successfully demonstrated that the PNA-immobilized fluorescent nanospheres (the colonoscopic imaging agent) recognized millimeter-sized colorectal tumors on the mucosal surface with high affinity and specificity in intestinal loop studies using human colorectal cancer orthotopic mouse models [11–12]. As expected, PNA and PNVA were necessary for specifically recognizing tumor tissues and preventing the nanospheres from interacting with normal tissues, respectively [15]. The nanosphere was a safe compound which remained locally on the luminal side of the large intestine. PNA immobilized on the nanosphere surface was stable in the intestinal lumen [13]. Furthermore, the nanospheres detected dynamic changes of the TF antigen in human colonic tissues from patients with colorectal tumors. However, theydid not bind to human colonic tissues from normal controls [16]. These data strongly supported the potential use of the PNA-immobilized fluorescent nanospheres for imaging the TF antigen as a biomarker for the early detection and prediction of the progression of colorectal cancer at the molecular level.

Our next target is to initiate clinical trials of the PNA-immobilized fluorescent nanospheres. Several issues must be still resolved for the initiation. The good manufacturing practice (GMP)-guided productivity is currently being evaluated. Toxicity studies are being conducted under a cooperation of contract laboratories having facilities that meet the good laboratory practice (GLP) specifications. We should also study imaging abilities of the PNA-immobilized fluorescent nanospheres in animal models that reflect the clinical disease. The study, which corresponds to pharmacological effects designated in the regulation, is required for predicting the clinical dose. However, it seems that the intestinal loop method used in our previous researches is not a suitable manner for the requirement. Here, we developed a mouse model which more resembled the clinical disease and subsequently evaluated the abilities of the PNA-immobilized fluorescent nanospheresto facilitate *in vivo* imaging of colorectal tumors using the model.

2. Results and discussion

2. 1. Characterization of nanospheres

A schematic representation of the PNA-immobilized fluorescent nanospheres is shown in Fig. 1. Coumarin 6 was encapsulated physicochemically into the polystyrene core of nanospheres with surface chains of PNVA and PMAA through their hydrophobic physicochemical interactions. PNA was anchored chemically to the polymeric platform (fluorescent nanospheres with surface chains of PNVA and PMAA) via the PMAA linker located on the nanosphere surface. Table 1 summarizes the characterization of PNA-

immobilized and lectin-free fluorescent nanospheres. Their physicochemical properties and the effects of various factors, such as the molecular weights of surface polymeric chains, on these properties have been thoroughly evaluated in our previous publication [10–11, 14].

2. 2. Human colorectal cancer orthotopic animal model

The PNA-immobilized fluorescent nanospheres were designed to recognize primary colon carcinoma-derived changes on the mucosal surface. Therefore, we needed an orthotopic animal model in which human colorectal cancer are exposed on the mucosal side of the large intestine. There are 2 types of human colorectal cancer orthotopic mouse models: (i) the implantation of cultured humancolorectal cancer cells in the large intestine [26];(ii) the implantation of fragments of tumor tissues in the large intestine [27]. However, neither of the models is satisfied with our requirements because cancer cells and tumor tissues are implanted on the serosal side of the intestine.

Since the mouse cecum is large and is not rigidly fixed in the abdomen, the implantation is easier compared to other segments of the large intestine. In our past studies [11–12], we have developed orthotopic mouse models bearing human colorectal tumors at the cecal mucosa and evaluated tumor recognition of the PNA-immobilized fluorescent nanospheres using the models. The model was based on the mucosal invasion of cancer cells and tumor tissues implanted on the serosal side of the cecum of nude and severe combined immunodeficiency (SCID) mice. HT-29, HCT-116, and LS174T cells were used as the TF antigen-expressing human colorectal cancer cells. The HT-29 and HCT-116 cells in which red fluorescent protein (RFP) gene was transduced (HT-29-RFPand HCT-116-RFP) were used to prepare tumor tissues. We have previously reported that these cancer cells and tumor tissues definitely invaded the mucosal side when the mice were maintained for several weeks after implantation although there was a difference in the period that was required for the mucosal invasion between experiments [11–12].

On the other hand, the cancer rarely develops in the cecal mucosa. In this study, an orthotopic nude mouse model bearing human colorectal tumors on the mucosa of the descending colon, which is one of frequent sites of this tumor, was newly developed. After HT-29 and HT-29-RFP cells were implanted on the serosal side of the descending colon of nude mice, the mice were maintained until the implanted cancer cells invaded the mucosal side. As shown in Table 2, the period that was required for the mucosal invasion was 4 weeks, regardless of RFP gene transduction. It was similar to the periods observed in our other orthotopic mouse models bearing human colorectal tumors at the cecal mucosa [11–12]. Using our new orthotopic mouse model, we subsequently evaluated abilities of the PNA-immobilized fluorescent nanospheres to facilitate in vivo imaging of colorectal tumors.

2. 3. *In vivo* imaging of colorectal tumors with the PNA-immobilized fluorescent nanospheres

We have previously proved the high affinity and specificity of the PNA-immobilized fluorescent nanospheres for colorectal tumors expressed at the cecal mucosa using the intestinal loop method. However, the intestinal loop method may overestimate the imaging efficacy of the nanospheres when compared with endoscopic observation in the clinic,

because the experimental conditions of the loop method are static and mild [11–12, 15]. In the present study, in order to more resemble the clinical situation, the dispersion of the PNA-immobilized fluorescent nanospheres was administered into the colonic lumen from the anus of the nude mice with human colorectal tumors at the mucosa of the descending colon. After the mice were maintained for a period, nanospheres that had not interacted with the colorectal tissues were drained from the lumen by injecting PBS into the colon. During the experiment, the entire colon was monitored in real-time using the *in vivo* imaging apparatus to demonstrate specific fluorescence of the colorectal tumor after the nanospheres were flushed. Our expectation is illustrated in Fig. 1. The PNA-immobilized fluorescent nanosphere-derived yellowish-green fluorescence will be observed along the descending colon after intracolonical administration (Fig. 1a). When PBS is injected into the intestinal lumen, most of nanospheres will drain away; however, yellowish-green fluorescence of nanospheres that bind to colorectal tumors will be observed. If the HT-29-RFP cells implantation model is tested, the nanospheres-derived yellowish-green fluorescence will overlap withthe HT-29-RFP cell-derived red fluorescence (Fig. 1b).

The intestinal loop study, which was previously performed to evaluate the tumor recognition of PNA-immobilized fluorescent nanospheres [12], revealed that the nanospheres detected colorectal tumors on the cecal mucosa within 1 min. The short time is indeed patient-friendly in the clinical site. The present study also gave similar results. We first evaluated nonspecific interactions using nude mice without tumors. As shown in Fig. 2 (a-1), the yellowish-green fluorescence of the PNA-immobilized fluorescent nanospheres was observed along the entire descending colon after the luminal side had been filled with the nanospheres. At 1 min following the intracolonical administration, 1 mL PBS was injected into the intestinal lumen at a rate of 0.1 mL/sec. As shown in Fig. 2 (b-1), no fluorescence was observed after washing the luminal side of the descending colon with PBS. This demonstrated that the fluorescent nanospheres were completely removed from the intestinal lumen even when mild washing processes were applied. A similar result was obtained when nude mice without tumors were maintained for 10 min following the intracolonical administration of the PNA-immobilized fluorescent nanospheres (data not shown). This indicated that the non-specific interactions were too weak to allow the imaging agent to remain on the normal colonic mucosa during the washing processes.

We next evaluated biorecognition of the PNA-immobilized fluorescent nanospheres using the orthotopic nude mice implanted with HT-29 cells. Yellowish-green fluorescence was observed along the entire descending colon after the luminal side had been filled with the nanospheres (Fig. 3a). The nanospheres were vigorously flushed with PBS. Most of the nanospheres were drained from the intestinal lumen. However, fluorescence was observed at the implantation site of cancer cells (Fig. 3b). As shown in Table 3 and Fig. 4a, histological evaluation demonstrated that colorectal cancer cells were present in the mucosal epithelia where the nanospheres fluoresced. The same test was performed for mice implanted with HT-29-RFPcells. As we expected (Fig. 1), the green fluorescence of the nanospheres overlapped with the HT-29-REP red fluorescence (Fig. 5). Histological evaluation also demonstrated that there was mucosal invasion of cancer cells at the site where the nanospheres' green fluorescence and HT-29-RFP red fluorescence co-localized (Table 3 and

Fig. 4b). We further evaluated behaviors of lectin-free fluorescent nanospheres with surface chains of PNVAin the large intestine of nude mice with orthotopic implantation of HT-29 cells. As shown in Fig. 6, the nanospheres without targeting moieties were completely removed from the intestine of the mouse bearing colorectal tumors through mild washing processes. No fluorescence was also observed at the normal mucosa that was far from the site in which cancer cells were implanted. The results were consistent with data obtained when interactions between lectin-free fluorescent nanospheres and colorectal tumors at the cecal mucosa were previously evaluated using the intestinal loop method [15].

We are currently planning to do *in vivo* endoscopic studies for small animals that pattern after clinical procedures. The study will be performed using a new animal model which we are currently making an effort to develop. In this model, the TF antigen-expressing cultured human colorectal cancer cells are implanted on the mucosal side of the descending colon in immunodeficiency small animals such as nude mice or nude rats. We are confident that this model is the most appropriate one for the evaluation of the PNA-immobilized fluorescent nanospheres because it clearly possesses the target antigen of the nanospheres and most closely imitate the development of colorectal tumors in humans. An objective of the *in vivo* endoscopic studies for which animal sacrifice will not be required is to make the dose dependency of the nanospheres clear. When the nanospheres are clinically used, they will be sprayed on the intestinal mucosa and maintained for a period that is required for biorecognition of the nanospheres for colorectal tumors. Nanospheres that do not interact with colorectal tumors will be subsequently washed out with adequate solvent under designated conditions. The nanospheres-bound colorectal tumors on the mucosal surface will be directly detected from the luminal side with a fluorescent endoscope. Using the mouse model developed here, the dose dependency was preliminary evaluated through observation of the nanospheres-bound colorectal tumors from the serosal side of the intestine. As shown in Fig. 7, fluorescent intensity of tumors recognized by the nanospheres decreased with the dose reduction. However, the fluorescence was detected from the serosal side by extending the exposure time even when the dose was set to 5 mg/mL. It is anticipated that a less amount of the nanospheres is sufficient for the tumor detection by the fluorescent endooscope because the nanospheres-bound tumors are observed directly from the mucosal side. Details in the dose dependency of the PNA-immobilized fluorescent nanospheres will be discussed in a future report.

3. Conclusions

This report indicated three important properties of the PNA-immobilized fluorescent nanospheres for clinical application: (i) The nanospheres that interact non-specifically with normal mucosa are easily removed through mild washing processes; (ii) The nanospheres recognize colorectal tumors within a short time; (iii) The nanospheres bind the tumors tightly even under severe washing conditions.

4. Experimental

4. 1. Materials

N-Vinylacetamide (NVA) monomers were from Showa Denko Co. (Tokyo, Japan). Coumarin 6 and PNA were obtained from Sigma-Aldrich (St. Louis, MO, USA). All other chemicals were commercial products of reagent grade.

The human colorectal adenocarcinoma cell line, HT-29, was purchased from Dainippon-Sumitomo Pharma Biomedical Co. Ltd. (Osaka, Japan). The HT-29 cell line in which red fluorescent protein (RFP) gene was transduced, HT-29-RFP, was purchased from AntiCancer Japan Inc. (Osaka, Japan). McCoy's 5A Medium, Modified (with sodium bicarbonate, without L-glutamine), RPMI-1640 Medium, Dulbecco's Phosphate Buffered Saline (PBS with $CaCl_2$ and $MgCl_2$), and Dulbecco's Phosphate Buffered Saline, Modified (PBS without divalent metal ions) were obtained from Sigma-Aldrich. Fetal bovine serum (FBS), penicillin (10,000 U/mL), streptomycin (10 mg/mL), L-glutamine (200 mM), and trypsin-EDTA (0.25% trypsin and 1 mM EDTA) were purchased from GIBCO Laboratories (Lenexa, KS, USA). Preserved rabbit blood and neuraminidase (sialidase, 1 unit/mL, extracted from *Arthrobacter ureafaciens*) were obtained from Nippon Bio-Test Laboratories Inc. (Tokyo, Japan) and Roche Diagnostics (Indianapolis, IN, USA), respectively.

4. 2. Preparation and characterization of nanospheres

A couple of of lectin-free nanospheres were prepared in the same manner as described previously [10–11]. Briefly, PNVA and poly(tert-butyl methacrylate) (PBMA) were prepared by the free radical polymerization of NVA and butyl methacrylate (BMA) monomers, respectively, in the presence of 2-mercaptoethanol. The resulting hydroxyl group-terminated PNVA and PBMA were reacted with *p*-chloromethyl styrene. Vinylbenzyl group-terminated poly(methacrylic acid) (PMAA) was obtained by hydrolyzing vinylbenzyl group-terminated PBMA in the presence of hydroquinone. Fluorescent nanospheres with surface chains of PNVA and PMAA (a precursor of the PNA-immobilized fluorescent nanospheres) were prepared by dispersion copolymerization between vinylbenzyl group-terminated PNVA, vinylbenzyl group-terminated PMAA, and styrene at a weight ratio of 1:1:2 in an ethanol/water mixture containing 2, 2'-azobisisobutyronitrile and coumarin 6 (0.1% of the total monomers). Vinylbenzyl group-terminated PNVA was copolymerized with styrene at a weight ratio of 1:1 to obtain other lectin-free fluorescent nanospheres with surface chains of PNVA. After the unreacted substances and unencapsulated coumarin 6 were removed by centrifugation, lectin-free nanospheres were dispersed in purified water at a concentration of 20 mg/mL. PNA was subsequently immobilized on the surface of fluorescent nanospheres with surface chains of PNVA and PMAA through the coupling of the amino groups of PNA with the carboxyl groups of PMAA activated by pre-incubation with 1-ethyl-3-(3-dimethylaminopropyl)carbodiimide. The resulting PNA-immobilized fluorescent nanospheres with surface PNVA chains (i.e., the PNA-immobilized fluorescent nanospheres) were purified through dialysis, and then dispersed in purified water at a concentration of 20 mg/mL.

Routine characterization of nanospheres was performed as described previously [10–11]. Briefly, weight- and number-average molecular weights (Mw and Mn) of PNVA and PMAA were determined by gel permeation chromatography. The size (weight-average diameter) of nanospheres was measured by dynamic light-scattering spectrophotometry. The zeta potential of nanospheres was measured by electrophoretic light-scattering spectrophotometry. The amount of coumarin 6 encapsulated into the nanosphere core was measured by spectrophotometry. The amount of PNA immobilized on the nanosphere surface was measured by the ninhydrin method. The affinity and specificity of immobilized PNA for recognition of Gal-β(1-3)GalNAc were evaluated using the hemagglutinationtest.

4. 3. Cell culture

HT-29 cells were seeded at a density of 6×10^4 cells/mL in a flask with a surface area of 75 or 150 cm^2. McCoy's 5A Medium, Modified supplemented with 10% (v/v) FBS, 50 U/mL penicillin, 50 μg/mL streptomycin, and 1.5 mM L-glutamine was used as a culture medium (25–75 mL). The cells were grown as a monolayer in the media and were maintained at 37°C in a humidified atmosphere of 95% O_2/5% CO_2. Cells were then routinely passaged when they became 100% confluent, and the low passage cells (passage: ≤10 times) were used. HT-29-RFP cells were cultured by procedure as described above, except that RPMI 1640 Medium, supplemented with 10% FBS (v/v) and 1.5mM L-glutamine was used as a culture medium.

4. 4.*In vivo* imaging study

4. 4. 1. Human colorectal cancer orthotopic mouse model—Animal studies were approved by the Ethical Review Committee of Setsunan University. All surgical procedures and animal manipulations were conducted under HEPA-filtered laminar-flow hoods.

Cultured cancer cells (HT-29 and HT-29-RFP) were washed with 20 mL of PBS (without divalent metal ions) after the removal of the culture media. PBS was removed, and the cells were treated at 37°C for 3 min with 2 mL of trypsin-EDTA solution. A corresponding culture medium (10 mL) was added to remove the cells from the flask. The collected cells were centrifuged at 180 g for 10 min, and the precipitated cells were suspended in PBS (with divalent metal ions) at a concentration of 1×10^6 cells/0.01 mL.

Nude mice (6-week-old outbred nu/nu female mice) were anesthetized with sodium pentobarbital. The surgical area was sterilized using ethanol (70%, v/v) and an incision approximately 1.5 cm long was made along the left lateral abdomen of the mouse using a pair of sterile scissors. After the abdomen was opened, the descending colon was exposed. The cell suspension (1×10^6 cells/0.01 mL) was injected into the colonic serosa of the mouse. The abdomen was then closed. Nude mice bearing colorectal tumors in the descending colon were maintained for a predetermined period until implanted cancer cells invaded the mucosal side of epithelial cells.

4. 4. 2. *In vivo* imaging of colorectal tumors—Nude mice bearing descending colon tumors were fasted for 24 h with free access to water before imaging experiments. Under pentobarbital anesthesia, the abdomen was opened and the entire colon was observed. The

PNA-immobilized fluorescent nanospheres and the lectin-free fluorescent nanospheres with surface chains of PNVA were dispersed in PBS (with divalent ions) at a concentration of 5–20 mg/mL and 20 mg/mL, respectively. The nanosphere dispersion was filled into a plastic feeding needle-attached syringe. The needle, whose tip was coated with rubber, was inserted into the anus of the mouse, and then 0.1 mL of the dispersion was administered intracolonically within ca. 1 sec. The luminal side of the descending colon including the area in which cancer cells were implanted was filled with the nanospheres. At 1–10 min after administration, an incision approximately 0.1 cm long was made at the transverse colon. The plastic feeding needle was inserted into the colon through the incision and ligated at the site. PBS (with divalent metal ions)-filled syringe was attached to the needle and PBS was injected into the colon. The volume of PBS and the injection rate was set to 1–5 mL and 0.1–1 mL/sec, respectively. During the experiment, the opened abdomen was monitored using an apparatus that can capture both brightfield and fluorescence images in real time (FluorVivo 300, INDEC BioSystems, Santa Clara, CA, USA). The excitation and emission wavelengths were set to 450–490 nm and > 510 nm, respectively. The detection was performed at an exposure of 1/20–1/5 of a second. The excitation and emission wavelengths were set to 500–540 nm and >570 nm, respectively, when HT-29-RFP-derived red fluorescencewas detected.

As a control, normal nude mice that did not undergo cancer cell implantation were tested in the same manner as described above.

4. 5. Histological Evaluation

The descending colon with the colorectal tumor was removed, divided into several pieces (less than 1 cm length), and fixed with a formaldehyde aqueous solution (10%, v/v). The tissue was sectioned at 3 μm-thickness at 200–300 μm intervals. The presence and absence of tumors on the mucosa was evaluated histologically using 3 slices that corresponded to positions at which the piece was divided equally in four parts.

Acknowledgments

This work was financially supported in part by a Grant-in-Aid from The Japan Society for the Promotion of Science (JSPS) and National Science Foundation (NSF) under the Japan-US cooperative Science Program (2009–2010) (for Shinji Sakuma (SS)), The Science Research Promotion Fund from The Promotion and Mutual Aid Corporation for Private Schools of Japan (2011–2012) (SS), The Japanese Foundation for Research and Promotion of Endoscopy (JFE, 2013) (SS), The National Cancer Institute R01 CA160700 (for Wellington Pham (WP)), and Vanderbilt Ingram Cancer Center (WP). The authors thank Showa Denko Co. for the donation of NVA monomers.

References

1. Tytherleigh MG, Warren BF, Mortensen NJ. Management of early rectal cancer. Br J Surg. 2008; 95:409–423.10.1002/bjs.6127 [PubMed: 18314929]
2. Siegel R, Naishadham D, Jamal A. Cancer statistics. CA Cancer J Clin. 2013; 63:11–30.10.3322/caac.21166 [PubMed: 23335087]
3. Young PE, Womeldorph CM. Colonoscopy for colorectal cancer screening. J Cancer. 2013; 4:217–226.10.7150/jca.5829 [PubMed: 23459594]
4. Moss A, Bourke MJ, Williams SJ, Hourigan LF, Brown G, Tam W, Singh R, Zanati S, Chen RY, Byth K. Endoscopic mucosal resection outcomes and prediction of submucosal cancer from

advanced colonic mucosal neoplasia. Gastroenterology. 2011; 140:1909–1918.10.1053/j.gastro.2011.02.062 [PubMed: 21392504]

5. Fukuzawa M, Saito Y, Matsuda T, Uraoka T, Itoi T, Moriyasu F. Effectiveness of narrow-band imaging magnification for invasion depth in early colorectal cancer. World J Gastroenterol. 2010; 16:1727–1734.10.3748/wjg.v16.i14.1727 [PubMed: 20380004]
6. Winawer SJ, Zauber AG, Ho MN, O'Brien MJ, Gottlieb LS, Sternberg SS, Waye JD, Schapiro M, Bond JH, Panish JF, Ackroyd F, Shike M, Kurtz RC, Hornsby-Lewis L, Gerdes H, Stewart ET. the National Polyp Study Workgroup; The National Polyp Study Workgroup. Prevention of colorectal cancer by colonoscopic polypectomy. N Eng J Med. 1993; 329:1977–1981.10.1056/NEJM199312303293701
7. Kudo S, Kashida H, Tamura T, Kogure E, Imai Y, Yamano H, Hart AR. Colonoscopic diagnosis and management of nonpolypoid early colorectal cancer. World J Surg. 2000; 24:1081–1090.10.1007/s002680010154 [PubMed: 11036286]
8. Mayer R, Wong WD, Rothenberger DA, Goldberg SM, Madoff RD. Colorectal cancer in inflammatory bowel disease: a continuing problem. Dis Colon Rectum. 1999; 42:343–347.10.1007/BF02236351 [PubMed: 10223754]
9. Hsiung PL, Hardy J, Friedland S, Soetikno R, Du CB, Wu AP, Sahbaie P, Crawford JM, Lowe AW, Contag CH, Wang TD. Detection of colonic dysplasia in vivo using a targeted heptapeptide and confocal microendoscopy. Nature Medicine. 2008; 14:454–458.10.1038/nm1692
10. Hiwatari K, Sakuma S, Iwata K, Masaoka Y, Kataoka M, Tachikawa H, Shoji Y, Yamashita S. Poly(N-vinylacetamide) chains enhance lectin-induced biorecognition through the reduction of nonspecific interactions with non-targets. Eur J Pharm Biopharm. 2008; 70:453–461.10.1016/j.ejpb.2008.04.027 [PubMed: 18577446]
11. Sakuma S, Yano T, Masaoka Y, Kataoka M, Hiwatari K, Tachikawa H, Shoji Y, Kimura R, Ma H, Yang Z, Tang L, Hoffman RM, Yamashita S. *In vitro*/*in vivo* biorecognition of lectin-immobilized fluorescent nanospheres for human colorectal cancer cells. J Control Release. 2009; 134:2–10.10.1016/j.jconrel.2008.10.017 [PubMed: 19014984]
12. Sakuma S, Yano T, Masaoka Y, Kataoka M, Hiwatari K, Tachikawa H, Shoji Y, Kimura R, Ma H, Yang Z, Tang L, Hoffman RM, Yamashita S. Detection of early colorectal cancer imaged with peanut agglutinin-immobilized fluorescent nanospheres having surface poly(N-vinylacetamide) chains. Eur J Pharm Biopharm. 2010; 74:451–460.10.1016/j.ejpb.2010.01.001 [PubMed: 20060903]
13. Sakuma S, Kataoka M, Higashino H, Yano T, Masaoka Y, Yamashita S, Hiwatari K, Tachikawa H, Kimura R, Nakamura K, Kumagai H, Gore JC, Pham W. A potential of peanut agglutinin-immobilized fluorescent nanospheres as a safe candidate of diagnostic drugs for colonoscopy. Eur J Pharm Sci. 2011; 42:340–347.10.1016/j.ejps.2010.12.011 [PubMed: 21216286]
14. Sakuma S, Yamashita S, Hiwatari K, Hoffman RM, Pham W. Lectin-immobilized fluorescent nanospheres for targeting to colorectal cancer from a physicochemical perspective. Curr Drug Discov Technol. 2011; 8:367–378.10.2174/157016311798109407 [PubMed: 21644921]
15. Sakuma S, Higashino H, Oshitani H, Masaoka Y, Kataoka M, Yamashita S, Hiwatari K, Tachikawa H, Kimura R, Nakamura K, Kumagai H, Gore JC, Pham W. Essence of affinity and specificity of peanut agglutinin-immobilized fluorescent nanospheres with surface poly(N-vinylacetamide) chains for colorectal cancer. Eur J Pharm Biopharm. 2011; 79:537–543.10.1016/j.ejpb.2011.06.001 [PubMed: 21693188]
16. Kumagai H, Pham W, Kataoka M, Hiwatari K, McBride J, Wilson K, Tachikawa H, Kimura R, Nakamura K, Liu E, Gore JC, Sakuma S. Multifunctional nanobeacon for imaging Thomsen-Friedenreich antigen-associated colorectal cancer. Int J Cancer. 2013; 132:2107–2117.10.1002/ijc.27903 [PubMed: 23055136]
17. Boland CR, Roberts JA. Quantitation of lectin binding sites in human colon mucins by use of peanut and wheat germ agglutinin. J Histochem Cytochem. 1988; 36:1305–1307.10.1177/36.10.3138307 [PubMed: 3138307]
18. Campbell BJ, Finnie IA, Hounsell EF, Rhodes JM. Direct demonstration of increased expression of Thomsen-Friedenreich (TF) antigen from colonic adenocarcinoma and ulcerative colitis mucin and its concealment in normal mucin. J Clin Invest. 1995; 95:571–576.10.1172/JCI117700 [PubMed: 7860740]

19. Sakuma S, Lu ZR, Kopečková P, Kopeček J. Biorecognizable HPMA copolymer-drug conjugates for colon-specific delivery of 9-aminocamptothecin. J Control Release. 2001; 75:365–379.10.1016/S0168-3659(01)00405-9 [PubMed: 11489323]
20. Wróblewski S, Berenson M, Kopečková P, Kopeček J. Potential of lectin-N-(2-hydroxypropyl)methacrylamide copolymer-drug conjugates for the treatment of pre-cancerous conditions. J Control Release. 2001; 74:283–293.10.1016/S0168-3659(01)00338-8 [PubMed: 11489508]
21. Schneider F, Kemmner W, Haensch W, Franke G, Gretschel S, Karsten U, Schlag P. Overexpression of sialyltransferase CMP-sialic acid: Galβ1,3GalNAc-R α6-sialyltransferase is related to poor patient survival in human colorectal carcinoma. Cancer Res. 2001; 61:4605–4611. [PubMed: 11389097]
22. Boland CR, Montgomery CK, Kim YS. A cancer-associated mucin alteration in benign colonic polyps. Gastroenterology. 1982; 82:664–672. [PubMed: 6800870]
23. Lotan R, Skutelsky E, Danon D, Sharon N. The purification, composition, and specificity of the anti-T lectin from peanut (Arachis hypogaea). J Biol Chem. 1975; 250:8518–8523. [PubMed: 811657]
24. Sakuma S, Sudo R, Suzuki N, Kikuchi H, Akashi M, Hayashi M. Mucoadhesion of polystyrene nanoparticles having surface hydrophilic polymeric chains in the gastrointestinal tract. Int J Pharm. 1999; 177:161–172.10.1016/S0378-5173(98)00346-9 [PubMed: 10205611]
25. Sakuma S, Hayashi M, Akashi M. Design of nanoparticles composed of graft copolymers for oral peptide delivery. Adv Drug Deliv Rev. 2001; 47:21–37.10.1016/S0169-409X(00)00119-8 [PubMed: 11251243]
26. Zamai M, vandeVen M, Farao M, Gratton E, Ghiglieri A, Castelli M, Fontana E, d'Argy R, Fiorino A, Pesenti E, Suarato A, Caiolfa V. Camptothecin poly[N-(2-hydroxypropyl)methacrylamide] copolymers in antitopoisomerase—I tumor therapy: intratumor release and antitumor efficacy. Mol Cancer Ther. 2003; 2:29–40.10.1186/1476-4598-2-29 [PubMed: 12533670]
27. Amoh Y, Yang M, Li L, Reynoso J, Bouvet M, Moossa AR, Katsuoka K, Hoffman RM. Nestin-linked green fluorescent protein transgenic nude mouse for imaging human tumor angiogenesis. Cancer Res. 2005; 65:5352–5357.10.1158/0008-5472.CAN-05-0821 [PubMed: 15958583]

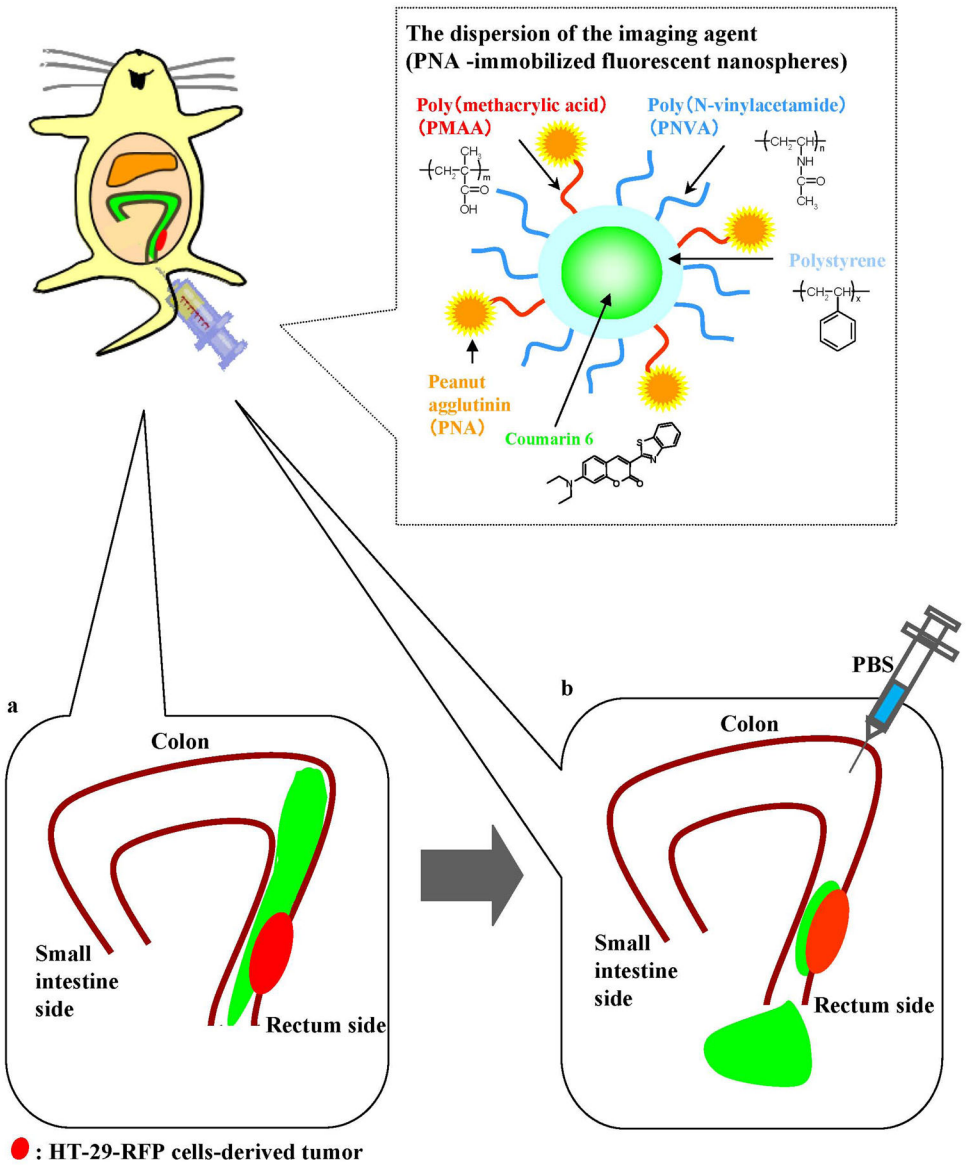

Fig 1.

Schematic representation of the experimental conditions for the in vivo imaging performed in this study.

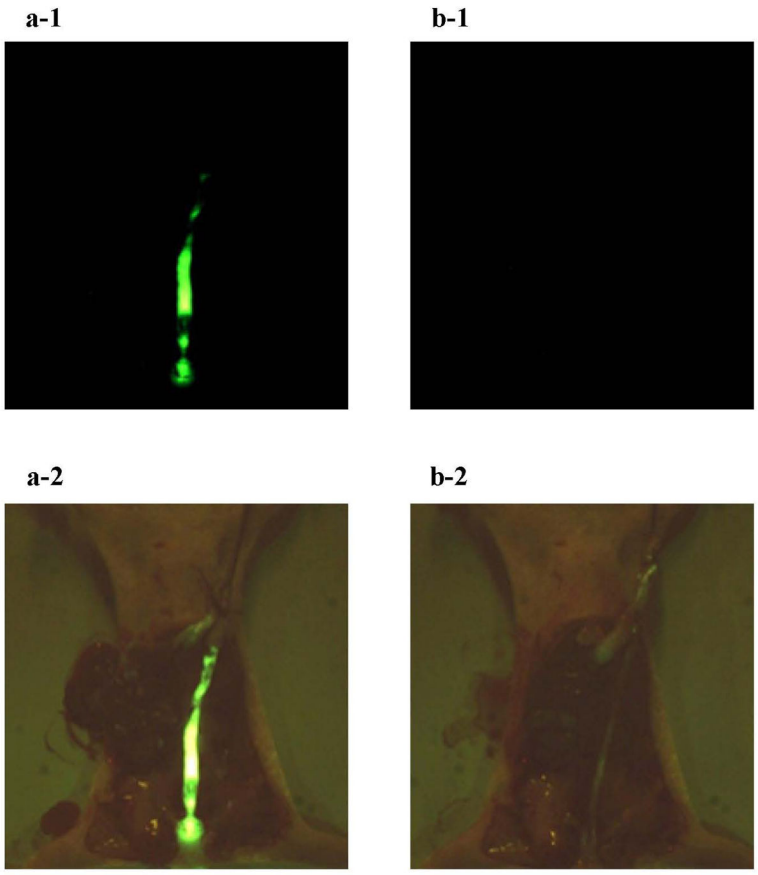

Fig 2.

Fluorescence images of the opened abdomen in the normal nude mouse. The PNA-immobilized fluorescent nanosphere dispersion (0.1 mL, 20 mg/mL) was intracolonically administered from the anus. One min after administration, the intestinal lumen was washed with 1 mL PBS (a small amount of PBS) at a rate of 0.1 mL/sec (a slow rate of PBS injection). Images a-1 and b-1 show fluorescence images of the opened abdomen before and after PBS washing, respectively (magnification: ×18; excitation: 450–490 nm; emission: > 510 nm; exposure: 1/20 second). Brightfield images (a-2 and b-2) were also obtained at the same site as the fluorescence images (magnification: ×18).

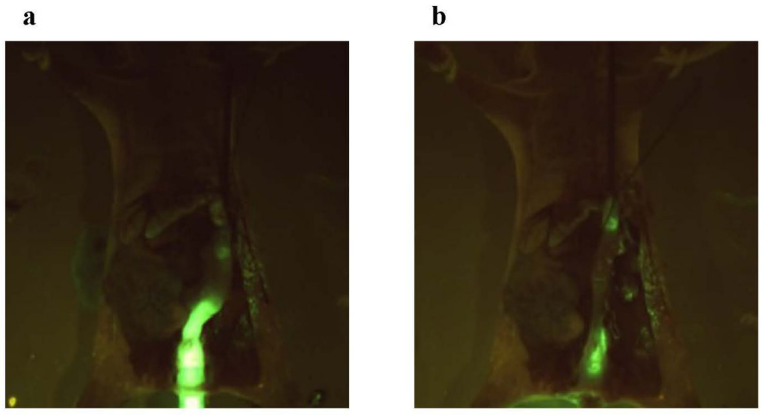

Fig 3.

Fluorescence images of the opened abdomen in the orthotopic HT-29 cell-implanted nude mouse that was maintained for > 4 weeks after cancer cells were implanted on the serosal side of the descending colon. The PNA-immobilized fluorescent nanosphere dispersion (0.1 mL, 20 mg/mL) was intracolonically administered from the anus. One min after administration, the intestinal lumen was washed with 5 mL PBS (a large amount of PBS) at a rate of 1 mL/sec (a fast rate of PBS injection). Images a and b show fluorescence images of the opened abdomen before and after PBS washing, respectively (magnification: ×18; excitation: 450–490 nm; emission: > 510 nm; exposure: 1/20 second).

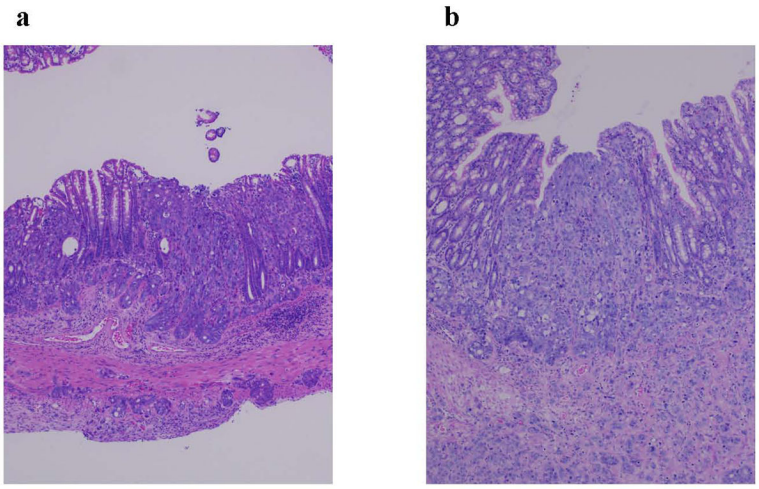

Fig 4.

Histological images of tissue pieces with the imaging agent-derived fluorescence exicised from the descending colon of cancer cell-implanted nude mice treated with the imaging agent (magnification: ×100). Images a and b corresponds to a sample of HT-29 cells-implanted descending colon (slice position: 2000 &m, Table 3) and a sample of HT-29-RFP cells-implanted descending colon (slice position: 5000 &m, Table 3), respectively.

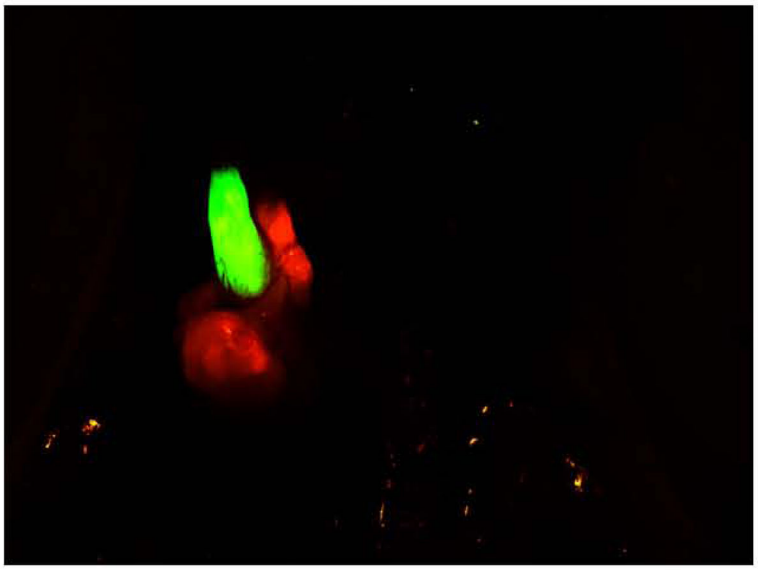

Fig 5.

Fluorescence images of the opened abdomen in the orthotopic HT-29-RFP cell-implanted nude mouse that was maintained for > 4 weeks after cancer cells were implanted on the serosal side of the descending colon. The PNA-immobilized fluorescent nanosphere dispersion (0.1 mL, 20 mg/mL) was intracolonically administered from the anus. One min after administration, the intestinal lumen was washed with 5 mL PBS at a rate of 1 mL/sec. Red fluorescence image of the HT-29-RFP cells-derived tumors (magnification: ×40; excitation: 500–540 nm; emission: > 570 nm; exposure: 1/20 second) was captured at the same position where yellowish green fluorescence image of the nanospheres (magnification: ×40; excitation: 450–490 nm; emission: > 510 nm; exposure: 1/20 second) was taken. Both images were overlapped.

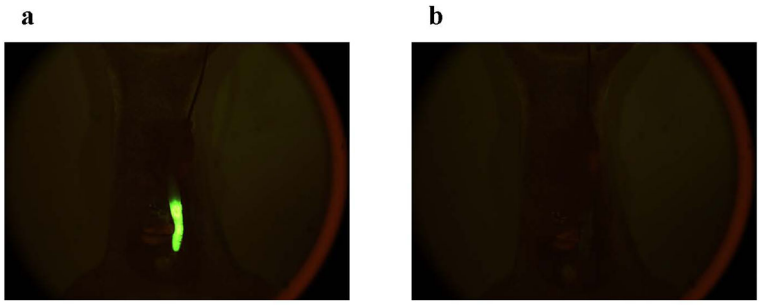

Fig 6.

Fluorescence images of the opened abdomen in the orthotopic HT-29 cell-implanted nude mouse that was maintained for > 4 weeks after cancer cells were implanted on the serosal side of the descending colon. The dispersion of lectin-free fluorescent nanospheres with surface chains of PNVA (0.1 mL, 20 mg/mL) was intracolonically administered from the anus. One min after administration, the intestinal lumen was washed with 1 mL PBS at a rate of 0.1 mL/sec. Images a and b show fluorescence images of the opened abdomen before and after PBS washing, respectively (magnification: ×18; excitation: 450–490 nm; emission: > 510 nm; exposure: 1/20 second).

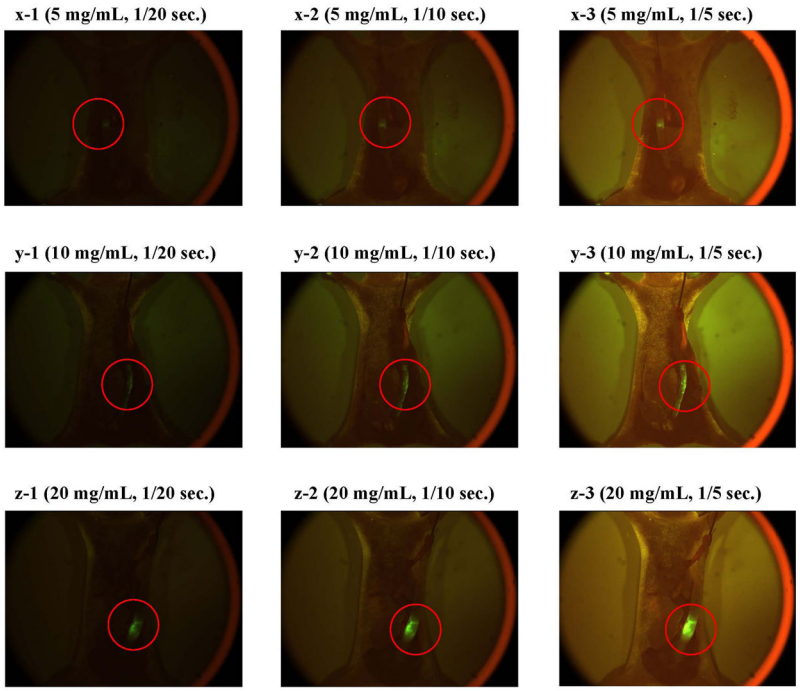

Fig 7.

Fluorescence images of the opened abdomen in the orthotopic HT-29 cell-implanted nude mice that were maintained for > 4 weeks after cancer cells were implanted on the serosal side of the descending colon (magnification: ×18; excitation: 450–490 nm; emission: > 510 nm; exposure: 1/20-1/5 second). The PNAimmobilized fluorescent nanosphere dispersion (0.1 mL) with a concentration of 5 mg/mL (x), 10 mg/Ml (y), amd 20 mg/mL (z) was intracolonically administered from the anus. One min after administration, the intestinal lumen was washed with 5 mL PBS at a rate of 1 mL/sec.

Table 1

Characterization of PNA-immobilized and lectin-free fluorescent nanospheres.

Characterization	PNA-immobilized fluorescent nanospheres	Lectin-free fluorescent nanospheres with PNVA and PMAA chains	Lectin-free fluorescent nanospheres with PNVA chains
Molecular weight of PNVA (Mw/Mn)	→	9500/4000	9500/4000
Molecular weight of PMAA (Mw/Mn)	→	10000/5600	-[h]
Particle size (nm)[a]	-[g]	302 ± 80	384 ± 90
Zeta potential (mV)[b]	-[g]	-21.8	-2.8
Encapsulated coumarin 6 (μg/mg)[c]	→	0.8	1.0
Immobilized PNA (μg/mg)[d]	6.6	-[h]	-[h]
Minimum conc. of PNA for agglutination of neuraminidase-treated erythrocytes (μg/mL)[e]	0.032	-[h]	-[h]
Minimum conc. of PNA for agglutination of neuraminidase-untreated erythrocytes (μg/mL)[f]	>33.0	-[h]	-[h]

[a] Weight-average diameter (mean ± s.d.)

[b] Measured in neutral PBS (without $CaCl_2$ and $MgCl_2$) at 25°C

[c] Encapsulated amount (μg) of coumarin 6 per milligram of the imaging agent and its precursor.

[d] Immobilized amount (μg) of PNA per milligram of the imaging agent.

[e] Minimum concentration of PNA immobilized on the nanospheres surface that induced neuraminidase-treated (Gal-β(1-3)GalNAc-expressed) erythrocyte agglutination.

[f] Minimum concentration of PNA immobilized on the nanospheres surface that induced neuraminidase-untreated erythrocyte agglutination.

[g] Not tested

[h] Not required

Contrast Media Mol Imaging. Author manuscript; available in PMC 2016 March 01.

Table 2

Histological evaluation of the descending colon of nude mice at 4 weeks after implantation of HT-29 and HT-29-RFP cells.

Samples	**HT-29 cells-implanted descending colon**			**HT-29-RFP cells-implanted descending colon**		
Slice position (μm)	**1000**	**4000**	**7000**	**850**	**3450**	**5950**
Lamina muscularis mucosae	+*	+*	+*	−	+*	+*
Lamina propria mucosae	+*	+*	+*	−	+*	+*
Mucosal epithelia	+	+	+	−	+	+

+ invasion of implanted cancer cells; −: no invasion;

* the invasion was observed in blood and/or lymph vessels

Table 3

Histological evaluation of tissue pieces with the imaging agent-derived fluorescence exicised from the descending colon of cancer cell-implanted nude mice treated with the imaging agent.

Samples	**HT-29 cells-implanted descending colon**			**HT-29-RFP cells-implanted descending colon**		
Slice position (μm)	**1000**	**2000**	**3000**	**2000**	**5000**	**8000**
Lamina muscularis mucosae	–*	–*	–*	+*	+*	+*
Lamina propria mucosae	+*	+*	+*	+*	+*	+*
Mucosal epithelia	+	+	+	–	+	+

+ invasion of implanted cancer cells; –: no invasion;

* the invasion was observed in blood and/or lymph vessels